

## Analytical Derivation of Interference Dips in Molecular Absorption Spectra: Molecular Properties and Relationships to Fano's Antiresonance

Daniel Neuhauser, Tae-Jun Park,\* and Jeffrey I. Zink

*Department of Chemistry and Biochemistry, University of California, Los Angeles, California 90095*

(Received 30 May 2000)

An analytical expression is derived for the decrease in the absorption cross section that occurs when two molecular electronic states are coupled by spin-orbit coupling. The loss of intensity, or interference dip, is common in the spectra of metal compounds. The derivation is based on a coupling of a single forbidden donor state to a broadened harmonic acceptor potential, and leads to simple analytical expressions. The new expressions give line shape functions different from those in the commonly used Fano antiresonance interpretation and are based on interpretable molecular properties.

PACS numbers: 31.10.+z, 33.20.-t

The spectra of metal-containing molecules and crystals often contain "interference dips," i.e., sharp decreases in absorbance at the energy of forbidden or weakly allowed intraconfigurational transitions [1–14]. The loss of absorbance is naively unexpected; the spectrum should consist of the superposition of the absorbances resulting from the transitions to the two different excited electronic states. The spectroscopic dips are routinely interpreted using the theory developed by Fano that was derived for atomic absorption in the presence of a slowly varying background continuum [15]. In molecular and crystal spectroscopy, however, the "background" contains an underlying dispersion part that varies strongly with energy [16–18]. It results from a dipole allowed electronic transition with a bandwidth determined by progressions in normal vibrational modes that are displaced between the excited and ground electronic states. A new treatment of the loss of absorbance that has physical relevance to molecules or to metal ions with strong phonon coupling to host lattices is needed.

In this Letter we derive a simple analytical expression for the intensity decrease and quantitatively interpret the phenomenon. The dips are a form of destructive quantum interference. The important molecular properties that govern the interference are the relative energies of the states, the vibrational frequencies in the electronic states, and the coupling properties.

Our analytical derivation uses the simplifying assumption that only one vibrational eigenstate of the "forbidden" electronic state is involved. This assumption is accurate for intraconfigurational transitions in metal compounds, where the spin multiplicity changes but the orbital configuration does not [19]. When this type of transition is well separated from more intense transitions, it is observed as a single line (i.e., little or no vibrational progression.) Our analytical expression for the interference dips is compared to the calculation using the full Hamiltonian.

The total electron-nuclear Hamiltonian for the coupled excited states is described in terms of the usual diabatic Hamiltonians [20]:

$$H = \frac{p^2}{2M} \begin{bmatrix} 1 & 0 \\ 0 & 1 \end{bmatrix} + \begin{bmatrix} \frac{1}{2} M \omega_F^2 x^2 + \varepsilon_F & \gamma \\ \gamma & \frac{1}{2} M \omega_0^2 (x - x_A)^2 + \varepsilon_A \end{bmatrix}, \quad (1)$$

where  $M$  is the oscillator's mass,  $\omega_0$  and  $\omega_F$  are the frequencies on the allowed and forbidden states,  $x$  is the vibrational coordinate,  $x_A$  is the shift of the vibrational-coordinate minimum upon excitation,  $\varepsilon_F$  and  $\varepsilon_A$  are the forbidden and allowed states' minimum potential, and  $\gamma$  is the off-diagonal coupling that is assumed to be coordinate independent. All energies are measured relative to the pre-excitation ground-state (electronic and vibrational) energy. The system is illustrated in Fig. 1, and the parameters used in the calculations are presented below.

The absorption cross section  $\sigma(\omega)$  as a function of frequency is given by

$$\begin{aligned} \sigma(\omega) &= \frac{1}{2\pi} \int_{-\infty}^{\infty} \langle \Psi_0 | e^{-i(H-\omega)t - i\Gamma|t|} | \Psi_0 \rangle dt \\ &= \frac{1}{\pi} \text{Im} \langle \Psi_0 | (H - \omega - i\Gamma)^{-1} | \Psi_0 \rangle. \end{aligned} \quad (2)$$

Here,  $\Gamma$  is a phenomenological (artificial) damping coefficient in the correlation function which approximately represents the effects of the coupling to other molecules or to the bath;  $\Psi_0$  is the initial wave function, which here is localized purely on the allowed state,  $\Psi_0 = [0, 1]^T \psi_0$ , and  $\psi_0(x)$  is the ground vibrational state of the ground electronic state. It is the same as the ground vibrational state of the forbidden excited state's Hamiltonian,  $p^2/2M + M\omega_0^2 x^2/2 + \varepsilon_F$ .

Numerically, the Hamiltonian in Eq. (1) is straightforward to invert so that the absorption probability can be calculated. For an analytical treatment, however, we make the following crucial approximation: Only *one* vibrational state (the ground state) of the forbidden electronic state is populated [17]. This approximation is justified because the

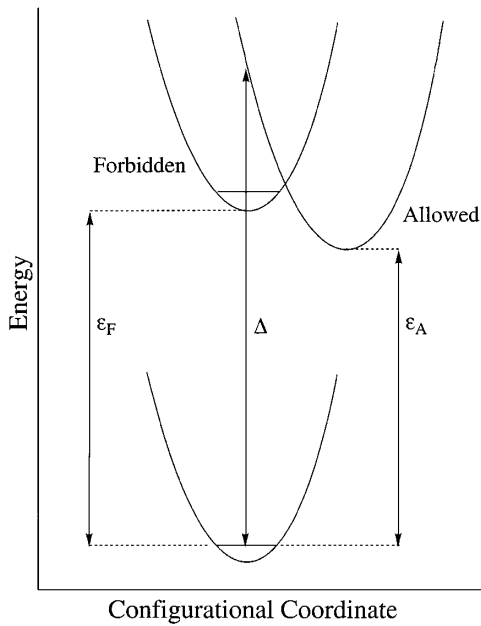


FIG. 1. Schematic diabatic potential energy surfaces that illustrate the model. The forbidden state is labeled “F”; the allowed state is labeled “A.”

excited vibrational states in the forbidden electronic state have zero overlap with the initial vibrational wave function. We also numerically verify this hypothesis; it is valid unless the coupling is much larger than the spacing.

With the single vibrational state on the donor, the resulting cross section can be shown straightforwardly to be [21,22] (Fig. 2)

$$\sigma(\omega) = -\frac{1}{\pi} \text{Im} \left( \frac{\beta}{1 - \gamma^2 \beta \alpha} \right), \quad (3)$$

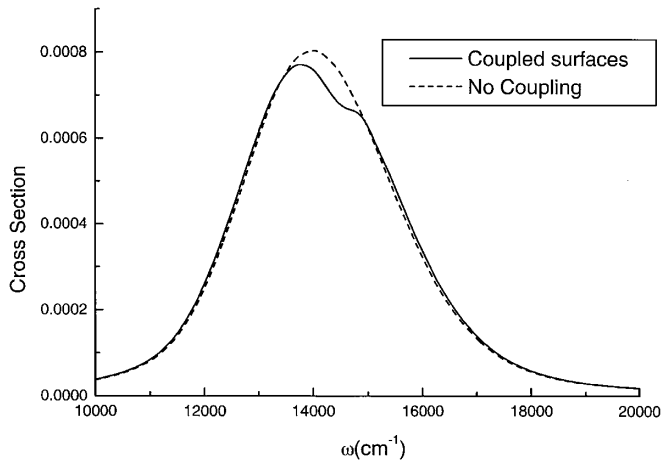


FIG. 2. Calculated absorption spectra (scaled by  $\pi$ ) with coupling (solid line) and without coupling (dashed line). The loss of intensity in the center of the spectrum (including coupling) is caused by the interference. Here, and in Figs. 3 and 4, the values used for the simulations are  $\omega_0 = \omega_F = 400 \text{ cm}^{-1}$ ,  $\Gamma = 450 \text{ cm}^{-1}$ ,  $\gamma = 300 \text{ cm}^{-1}$ ,  $\varepsilon_A = 10700 \text{ cm}^{-1}$ , and  $\varepsilon_F = 14200 \text{ cm}^{-1}$ .

where we defined the Green’s function for the single vibrational state (with energy  $\varepsilon_{F0} = \varepsilon_F + \omega_F/2$ ) on the forbidden states,

$$\alpha = 1/(\omega - \varepsilon_{F0} + i\Gamma), \quad (4)$$

while  $\beta$  is the expectation value of the Green’s function for the Hamiltonian  $H_A$  on the allowed state:

$$\beta = \left\langle \psi_0 \left| \frac{1}{E - H_A + i\Gamma} \right| \psi_0 \right\rangle. \quad (5)$$

Thus,  $\sigma_0(\omega) \equiv -\text{Im}\beta/\pi$  is simply the background absorption cross section, i.e., the spectrum resulting from a transition to the allowed state without the coupling to the forbidden state. Thus, when there is no coupling a smooth absorption is observed. Also, note that both  $\alpha$  and  $\beta$  are functions of frequency.

While  $\beta$  can be evaluated by a half-time Fourier transform of a simple analytical function, it is more illuminating to replace it by a simple Lorentzian-type function [23]:

$$\beta \approx \frac{1}{\omega - \Delta + i\sqrt{\omega_0\lambda}}. \quad (6)$$

The center of the Lorentzian is associated with the initial energy of the wave packet (Franck-Condon potential — see Fig. 1) and is at  $\Delta \equiv \varepsilon_A + \lambda$ , where  $\lambda = Mx_A^2/2$ . The width is associated with the slope of the harmonic potential on the allowed state and is approximately  $\sqrt{\omega_0\lambda}$ . The width is larger than the damping coefficient  $\Gamma$  in most molecules.

The crucial aspect of the Lorentzian is that its real part,  $\text{Re}\beta$ , changes phase at  $\omega = \Delta$ , i.e., at precisely the top of the zero-order absorption spectrum [ $\sigma_0(\omega)$ ]. Coupling of the allowed state to the forbidden state involves the dispersion part,  $\text{Re}\beta$ . Because it changes sign, it is not a constant background.

The analytic difference spectrum (plotted in Fig. 3), i.e., the difference between the spectrum with and without coupling, is

$$\sigma_{\text{diff}}(\omega) \equiv \sigma(\omega) - \sigma_0(\omega) = \frac{\gamma^2}{\pi} \text{Im} \left( \frac{\alpha \beta^2}{1 - \gamma^2 \beta \alpha} \right). \quad (7)$$

Note that the difference spectrum consists of two peaks separated by an interference dip. The mathematical reason for the double peak is most simply illustrated at low couplings, where the difference spectrum becomes  $\gamma^2 \text{Im}(\alpha \beta^2)/\pi$ , i.e.,

$$\sigma_{\text{diff}}(\omega) \approx \frac{\gamma^2}{\pi} \text{Im}(2 \text{Re}\alpha \text{Re}\beta \text{Im}\beta + \text{Im}\alpha \text{Re}\beta^2). \quad (8)$$

As shown in Figs. 3 and 4, the double peak is due to a product of the real parts (dispersion) of the Lorentzians,  $\text{Re}\alpha \text{Re}\beta$ , which changes signs in different parts of the spectrum. This term has two peaks; one below  $\min(\Delta, \varepsilon_{F0})$  and one above  $\max(\Delta, \varepsilon_{F0})$ . These peaks become two peaks in the overall difference spectrum: a

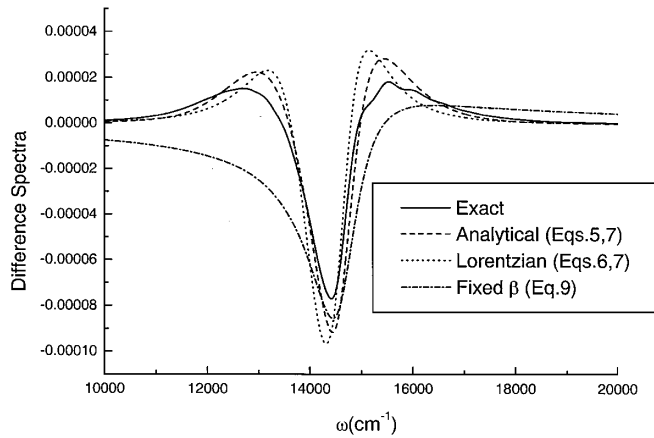


FIG. 3. Difference spectrum using both exact two-surface numerical calculations of Eq. (2), as well as analytical approximations [Eqs. (5) and (7)]—one using an exact calculation of  $\beta$  and one using a Lorentzian [Eqs. (6) and (7)]. Also included is a plot of a Fano-like spectrum obtained by using Eqs. (9)–(13) with  $\beta$  artificially fixed at its value for a frequency autoresonant with the transition to the dark state. All spectra scaled by  $\pi$ .

primary peak, associated with the usual Fano resonance near  $\varepsilon_{F0}$ , and a secondary peak, on the other side of the zero-order absorption peak, which is due to the flip in the sign of the dispersion part of the zero-order absorption. In contrast, for a truly slowly varying background (where  $\text{Re}(\beta)$  does not change sign) only one peak results. Thus, physically, the presence of the forbidden state acts coherently to reveal the varying phase of the dispersion part in the absorption spectrum.

We demonstrate these concepts by specific simulations, following earlier work where the Hamiltonian of Eq. (1) was explicitly evaluated using time-dependent techniques [19]. Specifically, we use frequencies of  $400 \text{ cm}^{-1}$  for both wells, and the shifting energy is  $\lambda = 3267 \text{ cm}^{-1}$ . The potential minima,  $\varepsilon_A$  and  $\varepsilon_F$ , are  $10700$  and

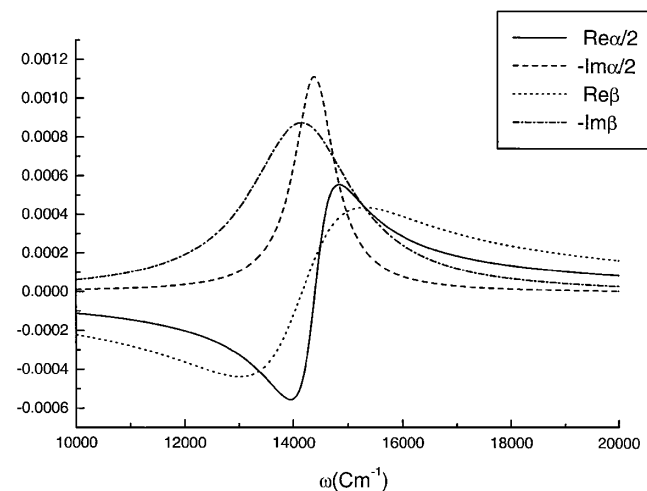


FIG. 4. Real and imaginary parts of  $\alpha$  and  $\beta$  [Lorentzian, Eq. (6)]. Constructive interference results when the real (dispersive) parts have the same sign. Arbitrary scale used.

$14200 \text{ cm}^{-1}$ , respectively. The system is relevant to ligand field excited states in metal complexes. The difference spectrum calculated using Eq. (7) compares well with that calculated using the full Hamiltonian, as shown in Fig. 3.

To emphasize the connection to previous analyses of interference dips in the spectra of transition metal and lanthanide metal systems, we write the absorption spectrum in an ostensibly equal form to Fano's relation:

$$\sigma(\omega) = \sigma_0(\omega) + g_0 \frac{q^2 + 2\xi q - 1}{1 + \xi^2}. \quad (9)$$

where a straightforward calculation shows that here

$$\xi = \frac{(\omega - \varepsilon_{F0} - \gamma^2 \text{Re}\beta)}{\eta}, \quad (10)$$

$$q = -\frac{\text{Re}\beta}{\text{Im}\beta} = \frac{\text{Re}\beta}{\pi\sigma_0}, \quad (11)$$

$$g_0 = \frac{\gamma^2 \pi (\sigma_0)^2}{\eta}, \quad (12)$$

and

$$\eta \equiv \Gamma + \gamma^2 \pi^2 \sigma_0. \quad (13)$$

We emphasize that this line shape is an exact reformulation of Eq. (7), but that the coefficients ( $q, \xi$ ) are frequency dependent. Fano's line shape results when  $\beta$  and therefore  $\sigma_0, q, \xi$  are fixed to be constant (as a function of frequency) in this formula. The Fano absorption correction term then gives a family of curves that depends on the value of  $q$ , the shape factor. The curves range from a Lorentzian function for  $|q| = \infty$  to an inverted Lorentzian for  $q = 0$ . For positive values of  $q$ , the spectrum shows destructive interference on the low energy side of the resonance, and vice versa. The “negative-positive” or “positive-negative” shape of the Fano correction (from low to high energy) is very different from the “positive-negative-positive” shape given by Eqs. (7) or (9) when we take into account the frequency dependence of  $\beta$ . This is illustrated in Fig. 3.

The underlying problem with most comparisons between experiment and theory is the necessity of choosing the “baseline” absorption spectrum,  $\sigma_0(\omega)$ , i.e., the expected spectrum when the coupling is zero. The typical choice is biased by the desire to use the Fano correction; for example, the background envelope is assumed to pass through the maximum to the high energy side of the band, thus artificially giving the negative-positive shape.

In summary, we note that both the analytical expression and the exact solution to the problem of interference dips show (Fig. 3) that the difference function will increase, decrease, and then increase again as the energy increases. In contrast, Fano's equation, applicable to a slowly varying background continuum, shows [Fig. 3, Eq. (9)] that the difference spectrum will increase and then decrease (or vice versa, depending on the sign of  $q$ ). Fano's equation

should not be used to calculate and interpret interferences in metal compounds.

We gratefully acknowledge discussions with Moshe Shapiro (D.N.) and support from NSF Grants No. CHE 9816552 (J.I.Z.) and No. CHE 9727084 (D.N.), from the Sloan Foundation (D.N.), and from the KOSEF Foundation (T.J.P.).

---

\*Permanent address: Chemistry Dept., Dongguk University, Seoul 100-715 Korea.

- [1] U. R. Rodriguez-Mendoza, V. D. Rodriguez, V. Lavin, I. R. Martin, and P. Nunez, *Spectrochim. Acta, Part A* **55**, 1319 (1999).
- [2] M. A. Noginov, G. B. Loutts, and M. Warren, *J. Opt. Soc. Am. B* **16**, 457 (1999).
- [3] M. A. Bunuel, R. Alcala, and R. Cases, *Solid State Commun.* **107**, 491 (1998).
- [4] M. A. Bunuel, R. Alcala, and R. Cases, *J. Chem. Phys.* **109**, 2294 (1998).
- [5] C. R. Mendonca, B. J. Costa, Y. Messaddeq, and S. C. Zilio, *Phys. Rev. B* **56**, 2483 (1997).
- [6] M. F. Hazenkamp, H. U. Guedel, M. Atanasov, U. Kesper, and D. Reinen, *Phys. Rev. B* **53**, 2367 (1996).
- [7] M. Voda, J. Garcia Sole, F. Jaque, I. Vergara, A. Kaminskii, B. Maill, and A. Butashin, *Phys. Rev. B* **49**, 3755 (1994).
- [8] A. Illarramendi, J. Fernandez, and R. Balda, *J. Chem. Phys.* **53**, 461 (1992).
- [9] R. G. McDonald, G. Robbie, R. Stranger, M. A. Hitchman, and P. W. Smith, *Chem. Phys.* **154**, 179 (1991).
- [10] J. L. Adam, P. Le Gall, and J. Lucas, *Phys. Chem. Glasses* **31**, 209 (1990).
- [11] A. Meijerink and G. Blasse, *Phys. Rev. B* **40**, 7288 (1989).
- [12] H. Riesen and H. U. Gudel, *Mol. Phys.* **60**, 1221 (1987).
- [13] A. Lempicki, L. Andrews, S. J. Nettel, B. C. McCollum, and E. I. Solomon, *Phys. Rev. Lett.* **44**, 1234 (1980).
- [14] M. D. Sturge, H. J. Guggenheim, and M. H. L. Pryce, *Phys. Rev. B* **2**, 2459 (1970).
- [15] U. Fano, *Phys. Rev.* **124**, 1866 (1961).
- [16] R. Kossloff and M. A. Ratner, *J. Chem. Phys.* **80**, 2352 (1984).
- [17] D. D. Druger, *J. Chem. Phys.* **67**, 3249 (1977).
- [18] A. Nitzan, *Mol. Phys.* **27**, 65 (1974).
- [19] D. F. Nelson and M. D. Sturge, *Phys. Rev.* **137**, 1117 (1965).
- [20] C. Reber and J. I. Zink, *J. Chem. Phys.* **96**, 2681 (1992).
- [21] See, e.g., W. H. Press, B. P. Flannery, S. A. Teukolsky, and W. T. Vetterling, *Numerical Recipes* (Cambridge University Press, Cambridge, UK, 1986).
- [22] T. J. Park, D. Neuhauser, and J. I. Zink (to be published).
- [23] D. J. Tannor and E. J. Heller, *J. Chem. Phys.* **77**, 202 (1982).